DOI: 10.3901/CJME.2016.0624.079, available online at www.springerlink.com; www.cjmenet.com

Elastoplastic Contact Mechanics Model of Rough Surface Based on Fractal Theory

YUAN Yuan[1,*], GAN Li[1], LIU Kai[1], and YANG Xiaohui[2]

1 *School of Mechanical and Precision Instrument Engineering, Xi'an University of Technology, Xi'an 710048, China*
2 *School of Mechanical Engineering, Xi'an Jiaotong University, Xi'an 710049, China*

Received October 21, 2015; revised June 21, 2016; accepted June 24, 2016

Abstract: Because the result of the MB fractal model contradicts with the classical contact mechanics, a revised elastoplastic contact model of a single asperity is developed based on fractal theory. The critical areas of a single asperity are scale dependent, with an increase in the contact load and contact area, a transition from elastic, elastoplastic to full plastic deformation takes place in this order. In considering the size distribution function, analytic expression between the total contact load and the real contact area on the contact surface is obtained. The elastic, elastoplastic and full plastic contact load are obtained by the critical elastic contact area of the biggest asperity and maximun contact area of a single asperity. The results show that a rough surface is firstly in elastic deformation. As the load increases, elastoplastic or full plastic deformation takes place. For constant characteristic length scale G, the slope of load-area relation is proportional to fractal dimension D. For constant fractal dimension D, the slope of load-area relation is inversely proportional to G. For constant D and G, the slope of load-area relation is inversely proportional to property of the material ϕ, namely with the same load, the material of rough surface is softer, and the total contact area is larger. The contact mechanics model provides a foundation for study of the friction, wear and seal performance of rough surfaces.

Keywords: rough surfaces, asperities, fractal theory, contact model

1 Introduction

Contact mechanics of rough surfaces has a significant impact on the phenomena of friction, wear, and lubrication as well as the conduction of heat and electricity. All engineered surfaces are microscopically rough, the contact between two rough surfaces is actually a series of contacts between the asperities, which leads to the real contact area being far less than the nominal contact area, carrying the capacity of conductive and heat conductivity per unit area according to the traditional contact theory has a certain amount of deviation with the actual situation, whereby resulting in premature failure of the normal working hours of contact elements. Therefore, how to characterize the relationship between the real contact area and the total contact load exactly is particularly important.

Much research work has been done on the description and contact analysis of rough surface by domestic and foreign scholars, who have mainly used the statistical analysis and the fractal theory, the former have used the statistical parameters which are scale-dependent to describe the contact behaviors of rough surfaces, resulting in the rough surface characterization and analysis of the result are not unique[1–3], the latter have used fractal parameters to characterize and simulate rough surfaces which are scale-independent to solve the problems[4–6]. MAJUMDAR, et al[4–5], developed the first fractal contact model(the MB model) using the Weierstrass and Mandelbrot fractal function(the WM function) and established the elastic, plastic regime of a single asperity. In considering the size distribution function in contact surface, the relations of the total contact load and the real contact area is obtained. However, the MB model ignores the elastoplastic deformation and holds that the critical contact area is scale independent. A transition from plastic to elastic contact occurs as the load and contact area increases. This phenomenon is essentially different from classical contact mechanics and seems to be impractical[7] Subsequently, many scholars have studied the mechanical properties of a single asperity in contact process and obtained the deformation mechanism which is contrary to the MB model. KOGUT, et al[8], used the finite element method to analyze the case of a single asperity contacting with a rigid flat surface(the KE model) and revealed three distinct stages that range from elasticity through elastoplasticity to full plasticity. MORAG, et al[7], presented a modified elastoplastic contact model of a single fractal asperity. The modified model showed the critical interference, the critical contact area and the critical load of a fractal single asperity are all scale dependent, with an increase in the load and contact area, a transition from elastic to plastic contact

* Corresponding author. E-mail: yuanytaurus@msn.com
Supported by National Natural Science Foundation of China(Grant Nos. 51105304, 51475364), and Shaanxi Provincial Natural Science Basic Research Plan of China(Grant No. 2015JM5212)

mode takes place in this order. LIOU, et al[9–11], proposed a revised elastoplastic contact model of a single fractal asperity, whose behaviors accord with classical contact mechanics. Then, the revised model can be applied to sphere-based and cylinder-based fractal bodies in contact with a rigid flat surface. MIAO, et al[12], suggested a revised contact model of a fractal rough surface by extending the modified asperity contact model developed by MORAG, et al[7]. In the model, the critical area of a single asperity is scale dependent so that the asperity's plastic to elastic model transition agrees with classical contact mechanics.

Above all, based on the former reseach solutions, an elastoplastic contact model of a single asperity is developed. According to the elastoplastic contact model, the critical contact areas of a single asperity are scale dependent. In considering the size distribution function, analytic expression between the total contact load and the real contact area on the contact surface is obtained. For the load-area analytic expression, the total contact load is only relevant to the maximun contact area of a single asperity. The elastic, elastoplastic and plastic contact load is obtained by the critical elastic contact area of the biggest asperity and maximun contact area of a single asperity, not to consider elastoplastic or full plastic deformation of a single asperity so that computational process is simplified.

2 Fractal Characterization of Rough Surface

MAJUMDAR, et al[4–5], have used the WM function to define a 2*D* multi-scale surface profile, the expression is

$$z(x)=G^{D-1}\sum_{n=n_{\min}}^{\infty}\frac{\cos(2\pi\gamma^n x)}{\gamma^{(2-D)n}}\quad (1<D<2,\ \gamma>1), \tag{1}$$

where $z(x)$ is the height of the surface profile, x is the shifting coordinates, D is the fractal dimension of the surface profile(for a physically continuous surface $1<D<2$), G is a characteristic length scale of the surface and γ^n determines the frequency spectrum of the surface.

These parameters to characterize the WM function are D, G, and $n_{\min}$, where $\gamma=1.5$ is found to be a suitable value for high spectral density and for phase randomization[4,7,13]. Since the rough surface is a non-stationary random process[14–15], the range of the index n indicating the frequency level is from $n_{\min}$(corresponding to the largest asperity determined by the length of the sample as $\gamma^{n_{\min}}=1/L$ [4–7]) to $n_{\max}$(corresponding to the smallest asperity determined by the resolution of the instrument). D and G can be found from the power spectrum of the WM function.

3 Fractal Contact Model

The contact between two rough surfaces can be simplified to an equivalent rough surface in contact with a rigid flat surface. These assumptions are as follows. The equivalent rough surface is isotropic and has fractal characteristics. Asperities are far away from one another so that there are no interactions between them, and no bulk deformation occurs during the contact. Work hardening due to contact, variation of material hardness with depth from the surface and the frictional force between the deformed asperities are neglected.

3.1 Mechanical model of a single asperity

According to the WM function, it is clear that the rough surface is composed of cosine waves of different wavelengths and amplitudes, superimposed on each other. For a wavelength of $l=1/\gamma^n$, the asperity shape before deformation is given as follows:

$$z_0(x)=G^{D-1}l^{2-D}\cos\frac{\pi x}{l}\quad\left(-\frac{l}{2}<x<\frac{l}{2}\right). \tag{2}$$

Fig. 1 shows the deformation of a single asperity, where l is the length scale(the base diameter) of a fractal asperity whose level is n, δ is the roughness amplitude, ω is the interference which is independent of δ and can range from zero to the amplitude($0\leqslant\omega\leqslant\delta$), l' is the truncation diameter, and l_r is the real contact diameter.

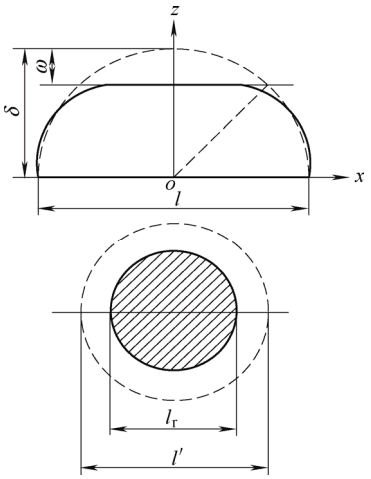

Fig. 1. Deformation of contacting asperities

The radius of curvature R at the tip of the asperity is

$$R=\left|\frac{\left(1+z'^2\right)^{3/2}}{z''}\right|_{x=0}=\frac{l^D}{\pi^2G^{D-1}}. \tag{3}$$

As Fig. 1 shown, the amplitude of the asperity δ is

$$\delta=z_0(0)=G^{D-1}l^{2-D}. \tag{4}$$

Hence, the interference ω is

$$\omega=\delta-z_0\left(\frac{l'}{2}\right)=G^{D-1}l^{2-D}\left[1-\cos\left(\frac{\pi l'}{2l}\right)\right]. \tag{5}$$

3.2 Regime of a single asperity

The deformation with a single asperity in contact with the rigid flat surface can be elastic, elastoplastic, or full plastic, and the existence conditions of a single asperity in three distinct deformation states are discussed.

3.2.1 Elastic deformation condition

According to the Hertz theory[16], the critical interference induced by a single asperity with a radius of R in contact with a smooth rigid flat surface is

$$\omega_{ec}=\left(\frac{\pi KH}{2E}\right)^2 R=\left(\frac{\pi K\phi}{2}\right)^2 R, \tag{6}$$

where H is the hardness of the softer material and K represents the hardness coefficient relating to the Poisson ratio υ of the material, namely K=0.454+0.41υ, E is the Equivalent Hertzian elastic modulus, $\phi=H/E$ is a property of the material.

When the interference $\omega=\omega_{ec}$, the single asperity is in elastic deformation. Because the radius of curvature of the asperity is far greater than the amplitude of the asperity, namely $R\gg\delta$ [5], the critical elastic contact area is

$$a_{ec}=\pi R\omega_{ec}=\pi\left(\frac{\pi K\phi}{2}\right)^2 R^2. \tag{7}$$

The elastic contact area can be expressed as

$$a=\pi R\omega. \tag{8}$$

Contrasting Eq. (7) and Eq. (8), we can be obtain that as the interference $\omega\leqslant\omega_{ec}$, the single asperity is in elastic deformation and the contact area belongs to $a\leqslant a_{ec}$. Substituting Eq. (3) into Eq. (7), the critical contact area can be written as

$$a_{ec}=\frac{1}{\pi}\left(\frac{K\phi}{2}\right)^2\left(\frac{l^D}{G^{D-1}}\right)^2. \tag{9}$$

The elastic contact load is

$$F=\frac{4}{3}ER^{1/2}\omega^{3/2}. \tag{10}$$

By using Eq. (8) and Eq. (10), the elastic contact load can be expressed as

$$F=\frac{4E\pi^{1/2}G^{D-1}}{3l^D}a^{3/2}. \tag{11}$$

The relations between the contact load and contact area in elastic deformation is $F\propto a^{3/2}$, and the solution is in agreement with the Hertz theory.

3.2.2 Elastoplastic deformation condition

KOGUT, et al[8], have conducted research on the elastoplastic deformation between a deformable hemisphere and a rigid flat surface using the finite element method. The result shows that for $\omega_{ec}<\omega\leqslant 110\omega_{ec}$, the hemisphere is in elastoplastic deformation which can be divided into two stages. When the interference ω meets with the requirement of $\omega_{ec}<\omega\leqslant 6\omega_{ec}$, the hemisphere is in the first elastoplastic deformation, or else the hemisphere is in the second elastoplastic deformation, namely $6\omega_{ec}<\omega\leqslant 110\omega_{ec}$.

The first critical elastoplastic interference ω_{epc} and the second critical elastoplastic interference ω_{pc} can be expressed as follows:

$$\omega_{epc}=6\omega_{ec}=6\left(\frac{\pi K\phi}{2}\right)^2 R, \tag{12}$$

$$\omega_{pc}=110\omega_{ec}=110\left(\frac{\pi K\phi}{2}\right)^2 R. \tag{13}$$

According to Eqs. (6), (12) and (13), the critical interferences are all dependent on the material property and the radius of curvature of the asperity. For same material, the radius of curvature is larger, the values of the critical interferences are greater.

3.2.2.1 The first elastoplastic deformation

As $\omega_{ec}<\omega\leqslant\omega_{epc}$, the single asperity is in the first elastoplastic deformation. The contact load and contact area can be written as follows:

$$F=\frac{2}{3}KH\pi R\omega_{ec}\times 1.03\left(\frac{\omega}{\omega_{ec}}\right)^{1.425}, \tag{14}$$

$$a=0.93\pi R\omega_{ec}\left(\frac{\omega}{\omega_{ec}}\right)^{1.136}. \tag{15}$$

Replacing ω in Eq. (15) with ω_{epc} in Eq. (12), the first critical elastoplastic contact area of a single asperity becomes

$$a_{epc}=0.93\pi R\omega_{ec}\left(\frac{\omega_{epc}}{\omega_{ec}}\right)^{1.136}=7.119\,7a_{ec}. \tag{16}$$

For $\omega_{ec}<\omega\leqslant\omega_{epc}$, we can obtain the contact area of a single asperity which belongs to $a_{ec}<a\leqslant a_{epc}$, the single asperity is in the first elastoplastic deformation. Therefore, Eq. (14) can be written as

$$F=\frac{2}{3}KH\times 1.1282\times a_{ec}^{-0.254\,4}a^{1.254\,4}. \tag{17}$$

Eq. (17) shows that in the first elastoplastic deformation, the load-area relation is $F \propto a^{1.254\,4}$.

3.2.2.2 The second elastoplastic deformation

As $\omega_{epc} < \omega \leqslant \omega_{pc}$, the single asperity is in the second elastoplastic deformation. The contact load and contact area can be written as follows:

$$F = \frac{2}{3} KH\pi R\omega_{ec} \times 1.40 \left(\frac{\omega}{\omega_{ec}}\right)^{1.263}, \tag{18}$$

$$a = 0.94\pi R\omega_{ec} \left(\frac{\omega}{\omega_{ec}}\right)^{1.146}. \tag{19}$$

Replacing ω in Eq. (19) with ω_{pc} in Eq. (13), the second critical elastoplastic contact area of a single asperity becomes

$$a_{pc} = 0.94\pi R\omega_{ec} \left(\frac{\omega_{pc}}{\omega_{ec}}\right)^{1.146} = 205.382\,7 a_{ec}. \tag{20}$$

For $\omega_{epc} < \omega \leqslant \omega_{pc}$, we can obtain the contact area of a single asperity which belongs to $a_{epc} < a \leqslant a_{pc}$, the single asperity is in the second elastoplastic deformation. Therefore, Eq. (18) can be written as

$$F = \frac{2}{3} KH \times 1.4988 \times a_{ec}^{-0.1021} a^{1.1021}. \tag{21}$$

Eq. (21) shows that in the second elastoplastic deformation, the load-area relation is $F \propto a^{1.1021}$.

3.2.3 Full plastic deformation condition

As $\omega > \omega_{pc}$, the single asperity is in full plastic deformation. The contact load and contact area can be written as follows[17]:

$$a = 2\pi R\omega, \tag{22}$$

$$F = Ha. \tag{23}$$

For $\omega > \omega_{pc}$, we can get $a > a_{pc}$, which means when the contact area of a single asperity is larger than the second critical elastoplastic contact area, the asperity is in full plastic deformation, the load-area relation is $F \propto a$.

These expressions are used to describe the relations between the contact area, contact load of an asperity and its interference in different states. The equations at critical points are discontinuity, the deviations are given as follows:

$$e_{a1} = \left|\frac{a_{ep1} - a_e}{a_e}\right|_{\omega=\omega_{ec}} \times 100\% = 7.00\%;$$

$$e_{F1} = \left|\frac{F_{ep1} - F_e}{F_e}\right|_{\omega=\omega_{ec}} \times 100\% = 3.00\%;$$

$$e_{a2} = \left|\frac{a_{ep2} - a_{ep1}}{a_{ep1}}\right|_{\omega=6\omega_{ec}} \times 100\% = 2.90\%;$$

$$e_{F2} = \left|\frac{F_{ep2} - F_{ep1}}{F_{ep1}}\right|_{\omega=6\omega_{ec}} \times 100\% = 1.68\%;$$

$$e_{a3} = \left|\frac{a_p - a_{ep2}}{a_{ep2}}\right|_{\omega=110\omega_{ec}} \times 100\% = 7.12\%;$$

$$e_{F3} = \left|\frac{F_p - F_{ep2}}{F_{ep2}}\right|_{\omega=110\omega_{ec}} \times 100\% = 9.20\%.$$

Where e is deviation, subscripts a and F represent the contact area and contact load and 1, 2, 3 reprsent the three critical points respectively. According to the calculation solutions, all of the deviations are less than 10% at the critical point so that the discontinuity effects can be ignored.

Above all, the critical contact areas(a_{ec}, a_{epc}, a_{pc}) are related not only to the material property and the fractal parameters, but also to the radius(R) of the asperity, As $a \leqslant a_{ec}$, the asperity is in elastic deformation. As $a_{ec} < a \leqslant a_{epc}$ the asperity is in the first elastoplastic deformation. As $a_{epc} < a \leqslant a_{pc}$, the asperity is in the second elastoplastic deformation. As $a > a_{pc}$, the asperity is in full plastic deformation.

3.3 Real contact area

WANG, et al[17], have noted that when a fractal rough surface contacts with a rigid flat surface, the size distribution function can be witten as

$$n(a) = \frac{D}{2} \varphi^{(2-D)/2} (a_L)^{D/2} (a)^{-(D+2)/2}. \tag{24}$$

Therefore the real contact area can be written as

$$A_r = \int_0^{a_L} n(a) a \mathrm{d}a = \frac{D}{2-D} \varphi^{(2-D)/2} a_L, \tag{25}$$

where a_L is the largest contact area, φ is the domain extension factor which is variable about D, satisfying the following formula:

$$\frac{\varphi^{(2-D)/2} - \left(1 + \varphi^{-D/2}\right)^{-(2-D)/D}}{(2-D)/D} = 1. \tag{26}$$

The real contact area of two contacted rough surfaces

includes elastic, the first elastoplastic, the second elastoplastic and the full plastic contact areas[18].

The real contact area can be written as

$$A_{\mathrm{r}} = A_{\mathrm{re}} + A_{\mathrm{rep1}} + A_{\mathrm{rep2}} + A_{\mathrm{rp}}\,, \tag{27}$$

where A_{re}, A_{rep1}, A_{rep2}, and A_{rp} represent the contact area for the elastic, the first elastoplastic, the second elastoplastic and the full plastic deformation respectively.

$$A_{\mathrm{re}} = \int_0^{a_{\mathrm{ec}}} n(a)a\mathrm{d}a = \frac{D}{2-D}\varphi^{(2-D)/2}a_{\mathrm{ec}}^{(2-D)/2}a_{\mathrm{L}}^{D/2}\,, \tag{28}$$

$$A_{\mathrm{rep1}} = \int_{a_{\mathrm{ec}}}^{a_{\mathrm{epc}}} n(a)a\mathrm{d}a = \frac{D}{2-D}\varphi^{(2-D)/2}\left[a_{\mathrm{epc}}^{(2-D)/2} - a_{\mathrm{ec}}^{(2-D)/2}\right]a_{\mathrm{L}}^{D/2}\,, \tag{29}$$

$$A_{\mathrm{rep2}} = \int_{a_{\mathrm{epc}}}^{a_{\mathrm{pc}}} n(a)a\mathrm{d}a = \frac{D}{2-D}\varphi^{(2-D)/2}\left[a_{\mathrm{pc}}^{(2-D)/2} - a_{\mathrm{epc}}^{(2-D)/2}\right]a_{\mathrm{L}}^{D/2}\,, \tag{30}$$

$$A_{\mathrm{rp}} = \int_{a_{\mathrm{pc}}}^{a_{\mathrm{L}}} n(a)a\mathrm{d}a = \frac{D}{2-D}\varphi^{(2-D)/2}\left[a_{\mathrm{L}}^{(2-D)/2} - a_{\mathrm{pc}}^{(2-D)/2}\right]a_{\mathrm{L}}^{D/2}\,, \tag{31}$$

According to Eq. (25), the real contact area is only dependent on the largest contact area a_{L}, nothing to do with the critical contact areas because the critical contact area is incorporated out. From Eq. (27), A_{re}, A_{rep1}, A_{rep2}, and A_{rp} are dependent on the critical contact areas(a_{ec}, a_{epc}, a_{pc}) and the largest contact area a_{L}. In the MB model, the critical contact area is scale-independent, that is, it is a constant for any asperity. In the present model, the critical contact areas of a single asperity are scale-dependent, they are vairiable for asperities whose levels is different. In general, the critical contact areas(a_{ec}, a_{epc}, a_{pc}) are corresponding to the largest contact area a_{L} from initial contact to complete contact. Accordingly the rationality of the selection is discussed in the following.

For these asperities whose levels range from $n_{\min}$ to $n_{\max}$, the asperity whose level is $n_{\min}$ is the biggest asperity and the asperity whose level is $n_{\max}$ is the smallest asperity. From initial contact to complete contact, the asperity whose level is $n_{\min}$ possesses the maximum contact area with a same interference, namely $a_{\mathrm{L}(n_{\min})} > a_{\mathrm{L}(n_{\min}+1)} > \cdots > a_{\mathrm{L}(n_{\max})}$. When the asperities in each level are completely deformed, we can obtain the ratio of contact areas between two different levels asperities:

$$\frac{a_{\mathrm{L}(n+i)}}{a_{\mathrm{L}(n)}} = \left(\frac{l_{n+i}}{l_n}\right)^2 = \left(\frac{1}{\gamma^i}\right)^2 \quad (i = 1,2,\cdots,N)\,, \tag{32}$$

where $a_{\mathrm{L}(n+i)}$ and $a_{\mathrm{L}(n)}$ represent the contact area at level $n+i$ and at level n respectively. For $\gamma = 1.5$, $i = 1$ the ratio equals 44.44%. For $i = 2$, the ratio equals 19.75%. When $i \geqslant 3$, the ratio will less than 8.779%. Above all, for certain interference, the largest contact area in the biggest asperity and the critical contact areas are corresponding to the biggest asperity.

3.4 Total contact load

According to the real contact area, the total contact load can be written as follows:

$$F_{\mathrm{r}} = F_{\mathrm{re}} + F_{\mathrm{rep1}} + F_{\mathrm{rep2}} + F_{\mathrm{rp}}\,, \tag{33}$$

where F_{re}, F_{rep1}, F_{rep2}, and F_{rp} represent the contact load for the elastic, the first elastoplastic, the second elastoplastic and the full plastic deformation respectively.

$$F_{\mathrm{re}} = \int_0^{a_{\mathrm{ec}}} Fn(a)\mathrm{d}a = \frac{D}{3-D}\varphi^{(2-D)/2}\frac{4E\pi^{1/2}G^{D-1}}{3l^D}a_{\mathrm{ec}}^{(3-D)/2}a_{\mathrm{L}}^{D/2}\,, \tag{34}$$

$$F_{\mathrm{rep1}} = \int_{a_{\mathrm{ec}}}^{a_{\mathrm{epc}}} Fn(a)\mathrm{d}a = \frac{D}{3}KH\times\varphi^{(2-D)/2}\times \frac{1.2816a_{\mathrm{ec}}^{-0.2544}}{1.425-0.568D}\left[a_{\mathrm{epc}}^{1.2544-0.5D} - a_{\mathrm{ec}}^{1.2544-0.5D}\right]a_{\mathrm{L}}^{D/2}\,, \tag{35}$$

$$F_{\mathrm{rep2}} = \int_{a_{\mathrm{epc}}}^{a_{\mathrm{pc}}} Fn(a)\mathrm{d}a = \frac{D}{3}KH\times\varphi^{(2-D)/2}\times \frac{1.7176a_{\mathrm{ec}}^{-0.1021}}{1.263-0.573D}\left[a_{\mathrm{pc}}^{1.1021-0.5D} - a_{\mathrm{epc}}^{1.1021-0.5D}\right]a_{\mathrm{L}}^{D/2}\,, \tag{36}$$

$$F_{\mathrm{rp}} = \int_{a_{\mathrm{pc}}}^{a_{\mathrm{L}}} Fn(a)\mathrm{d}a = \frac{HD}{2-D}\varphi^{(2-D)/2}\left[a_{\mathrm{L}}^{(2-D)/2} - a_{\mathrm{pc}}^{(2-D)/2}\right]a_{\mathrm{L}}^{D/2}\,. \tag{37}$$

Substituting Eqs. (34)–(37) into (33) can obtain the relation between the total contact load and the real contact area in dimensionless form:

$$F_{\mathrm{r}}^* = \frac{4\pi^{1/2}G^{*(D-1)}}{3l^{*D}}g_1(D)a_{\mathrm{ec}}^{*(3-D)/2}A_{\mathrm{r}}^{*D/2} + \frac{D}{3}K\phi g_2(D)\times \frac{1.281\,6a_{\mathrm{ec}}^{*-0.2544}}{1.425-0.568D}\left[a_{\mathrm{epc}}^{*(1.254\,4-0.5D)} - a_{\mathrm{ec}}^{*(1.254\,4-0.5D)}\right]A_{\mathrm{r}}^{*D/2} + \frac{D}{3}K\phi g_2(D)\frac{1.717\,6a_{\mathrm{ec}}^{*-0.1021}}{1.263-0.573D}\left[a_{\mathrm{pc}}^{*(1.254\,4-0.5D)} - a_{\mathrm{epc}}^{*(1.254\,4-0.5D)}\right]A_{\mathrm{r}}^{*D/2} + \frac{\phi}{g_3(D)}\left[g_3(D)A_{\mathrm{r}}^{*(2-D)/2} - a_{\mathrm{pc}}^{*(1.254\,4-0.5D)}\right]A_{\mathrm{r}}^{*D/2}\,, \tag{38}$$

where $F_{\mathrm{r}}^* = \dfrac{F_{\mathrm{r}}}{EA_{\mathrm{a}}}$, $l^* = \dfrac{l_{\max}}{\sqrt{A_{\mathrm{a}}}}$, $G^* = \dfrac{G}{\sqrt{A_{\mathrm{a}}}}$, $A_{\mathrm{r}}^* = \dfrac{A_{\mathrm{r}}}{A_{\mathrm{a}}}$,

$$a_{ec}^{*}=\frac{a_{ec}}{A_a},\ a_{epc}^{*}=\frac{a_{epc}}{A_a},\ a_{pc}^{*}=\frac{a_{pc}}{A_a}$$

are the dimesionless parameters; l_{max} is the size of the maximum asperity, A_a represents the nominal contact area,

$$g_1(D)=\frac{D}{3-D}\left(\frac{2-D}{D}\right)^{D/2}\varphi^{(D-2)^2/4};$$

$$g_2(D)=\left(\frac{2-D}{D}\right)^{D/2}\varphi^{(D-2)^2/4};$$

$$g_3(D)=\left(\frac{2-D}{D}\right)^{(2-D)/2}\varphi^{-(D-2)^2/4}.$$

4 Results and Discussion

Based on the former calculation results, the mechanical properties of the rough surface in contact process is analyzed in this chapter. Related parameters are shown in Table 1[3, 19].

Table 1. Calculation parameters of the surface

Related parameter	Value
Nominal contact area A_a / m^2	9×10^{-12}
Fractal dimension D	1.1, 1.3, 1.5, 1.7, 1.9
Fractal roughness parameter G / m	$2.5\times(10^{-7}, 10^{-8}, 10^{-9})$
Material property ϕ	10^{-2}, 10^{-3}, 10^{-4}
Poisson ratio υ	0.3
The size of the maximum asperity l_{max} / um	1
The resolution of the instrument L_s / nm	1

Fig. 2 shows the relation between critical areas and radius of curvature. For same radius of curvature, the elastic critical area is minimum, the second elastoplastic critical area is maximum, first elastoplastic critical area is between them. When the radii of curvature are different, these critical areas are proportional to radii of curvature. When a single asperity is under contact load, elastic deformation firstly takes place. As the load increases, elastoplastic and full plastic deformation will take place consequently. These solutions accord with classical contact mechanics.

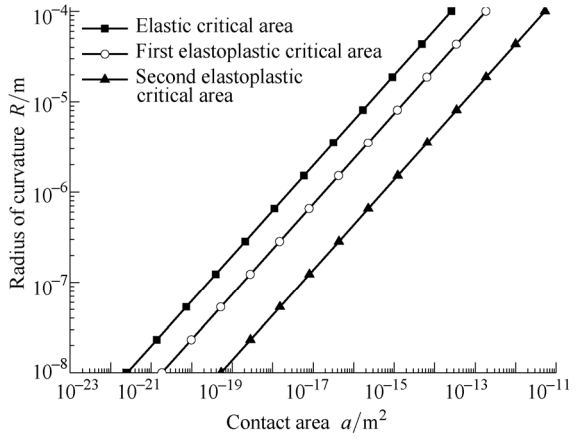

Fig. 2 Relation between critical areas and radius of curvature

Figs. 3(a), (b) and (c) show the relations between the dimensionless contact load and the dimensionless contact area in the stage of elastic, elastoplastic and full plastic deformation respectivily for different values of D. In elastic stage, the load-area relation is $F_r^* \propto A_r^{*3/2}$. In elastoplastic stage, the load-area relation is $F_r^* \propto A_r^{*1.254\,4}$ or $F_r^* \propto A_r^{*1.102\,1}$. In full plastic stage, the load-area relation is $F_r^* \propto A_r^*$. Because the ratio of elastic and elastoplastic stage to full plastic stage is small, the load-area relation is approximately linear. As the fractal dimension D increases, the slope of the load-area curve is increasing. This phenomenon shows that as the fractal dimension D increases, the profile of the rough surface is more complex and the number of asperity is much more. For a same contact load, the real contact area is proportional to the fractal dimension D.

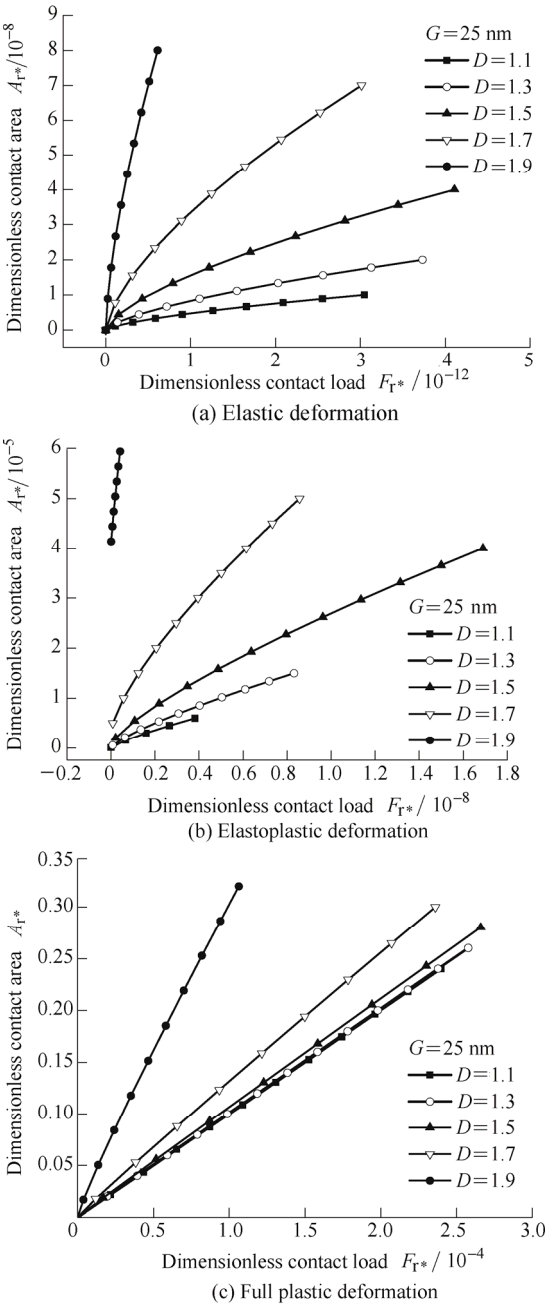

Fig. 3 Relations between the dimensionless contact area and the dimensionless contact load for different values of D

Figs. 4(a), (b) and (c) show the relations between the dimensionless contact load and the dimensionless contact area in the stage of elastic, elastoplastic and full plastic deformation respectivily for different values of G. The load-area relation is similar to those in Fig. 3. As the characteristic length scale G increases, the slope of the load-area curve is decreasing. When the characteristic length scale G increases, the height of a single asperity grows and the radius of curvature decreases. For a same contact load, the real contact area is inversely proportional to the G.

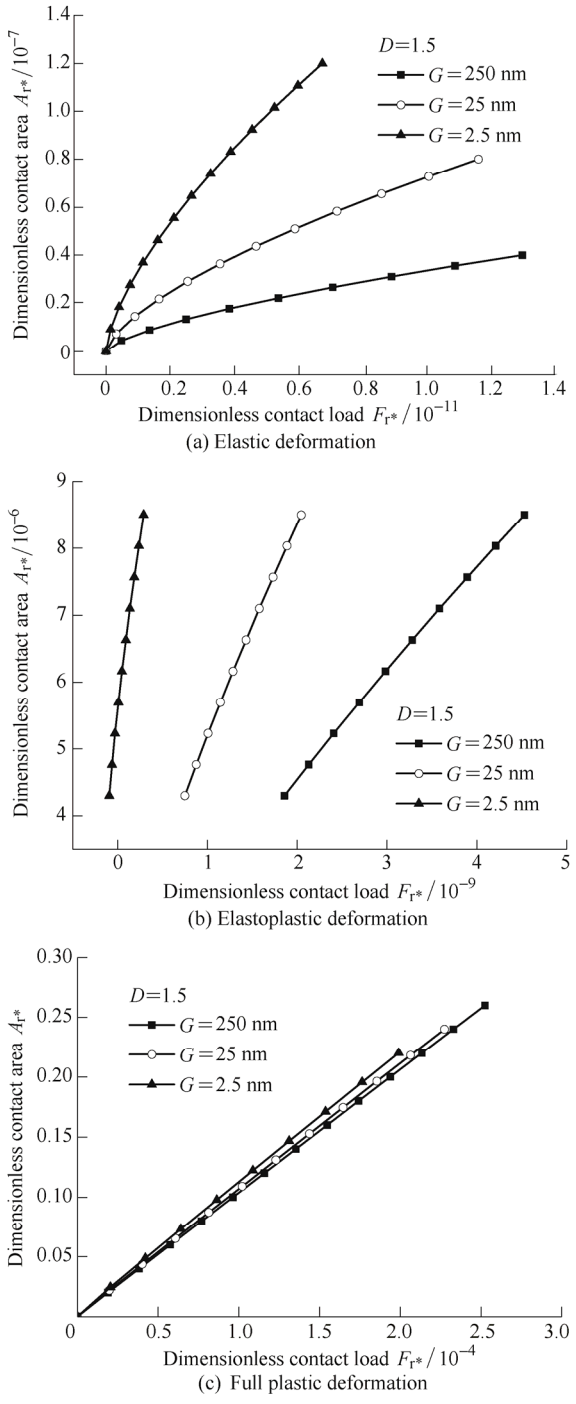

Fig. 4 Relations between the dimensionless contact area and the dimensionless contact load for different values of G

Figs. 5(a), (b) and (c) show the relations between the dimensionless contact load and the dimensionless contact area in the stage of elastic, elastoplastic and full plastic deformation for different values of ϕ respectivily. The load-area relation is similar to those in Fig. 3. With the property of the material ϕ increases, the slope of the load-area curve is decreasing, namely with the same load, the material of rough surface is softer, the total contact area is larger.

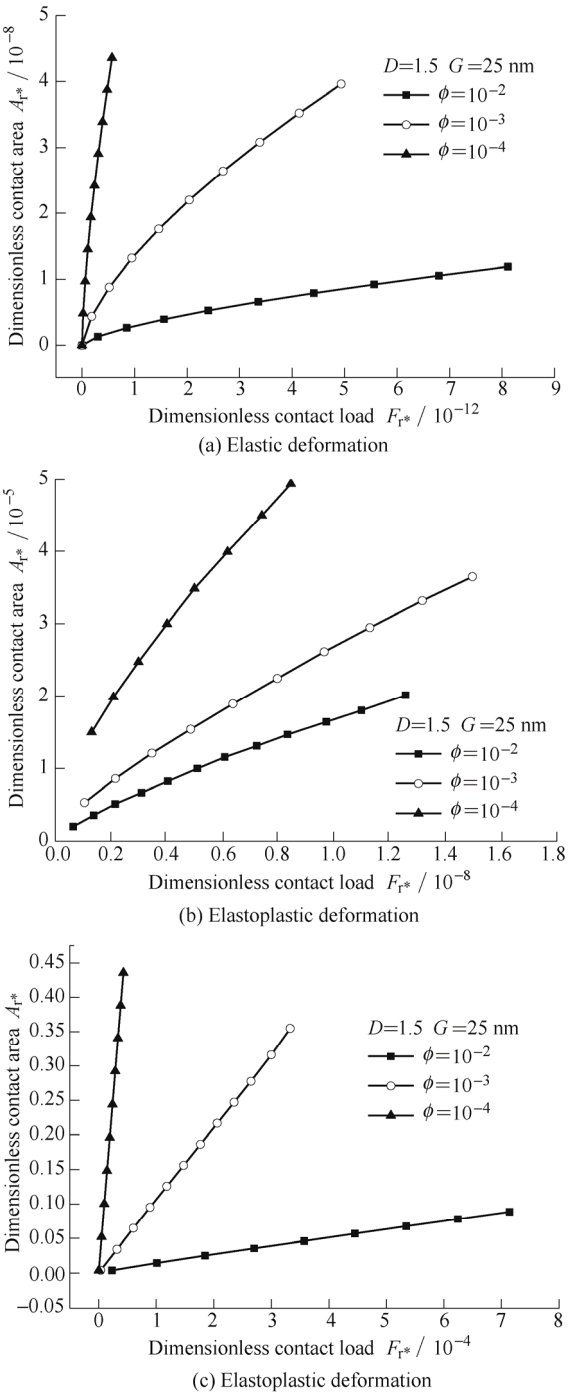

Fig. 5 Relations between the dimensionless contact area and the dimensionless contact load for different values of ϕ

Fig. 6 presents the ratios of elastic contact area to real contact area for different values of D. For a certain fractal dimension D, rough surface is first in elastic deformation under contact load. In this stage, the real contact area

equals to the elastic area, so that $A_{re}/A_r=1$. As the contact load increases, elastoplastic deformation takes place, elastic area becomes less than real contact area. The ratio of elastic contact area to real contact area is gradually decreasing and approaches to zero. As the fractal dimension D increases, the radius of curvature of asperity grows, so that the elastic area of rough surface enlarges. The ratio of elastic contact area to real contact area with D=1.9 is greater than ratios of which D=1.1 and D=1.5.

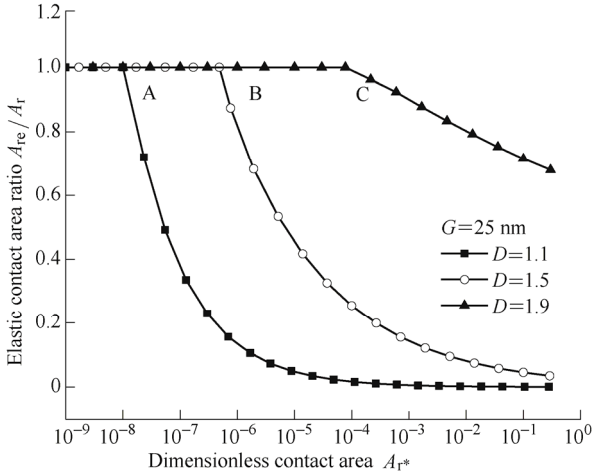

Fig. 6 Ratios of elastic contact area to real contact area for different values of D

Fig. 7 shows the ratios of elastoplastic contact area to real contact area for different values of D. When the rough surface is in elastic deformation, the elastoplastic contact area equals to zero, $A_{rep}/A_r=0$. As the contact load increases, elastoplastic deformation takes place in the rough surface. A_{rep}/A_r is gradually increasing which range from 0 to 1. In the second elastoplastic deformation stage, elastoplastic contact area is much greater than elastic contact area, A_{rep}/A_r approaches to 1. As the full plastic deformation initially takes place, A_{rep}/A_r reaches the maximum value, and then, A_{rep}/A_r is gradually decreasing. As the fractal dimension D increases, A_{rep}/A_r is similar to those in Fig. 6.

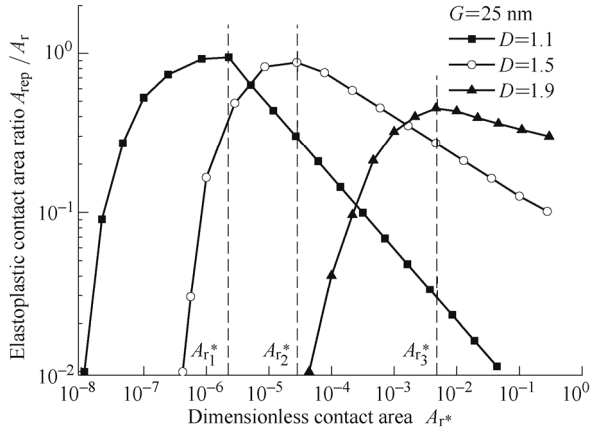

Fig. 7 Ratios of elastoplastic contact area to real contact area for different values of D

5 Comparison with Other Models

Fig. 8 shows the comparison between the present fractal model and other models such as GW model[1], MB model[4] and the experiment data of BHUSHAN[20], where D=1.49, $G^*=10^{-10}$ and $\phi=0.05$. It can be observed that there is a same tendency between the present fractal model and other models, whose dimensionless contact area is proportional to dimensionless contact load. Noting that for $F_r^*<2\times10^{-5}$, the present fractal model and MB model are in agreement with experimental data. As $2\times10^{-5}<F_r^*<2.5\times10^{-5}$, MB model is in agreement with the experimental data. As $2.5\times10^{-5}<F_r^*<5\times10^{-5}$, the present fractal model is in excellent agreement with experimental data, MB model and the GW model have some deviations. As $5\times10^{-5}<F_r^*<8\times10^{-5}$, the deviations between the GW model and the experimental data are the least. The results indicate that at the low and medium loads, the present fractal model is better than the statistics model, and at high loads, the statistical results are more accurate.

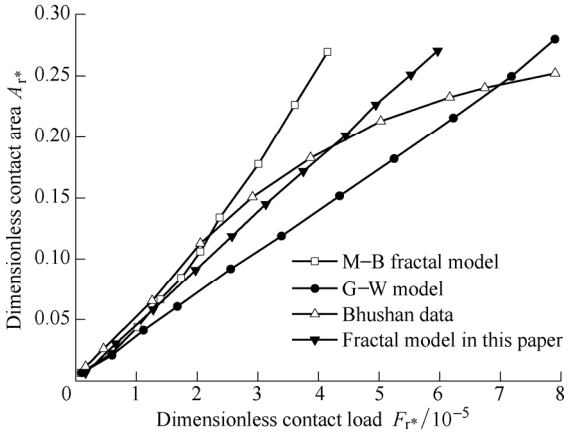

Fig. 8 Comparison between the present fractal model and other models[21]

6 Conclusions

(1) The critical interferences, the critical contact areas and the critical loads of a fractal single asperity are all scale dependent. For a constant material property, the critical contact areas are proportional to the square of the radius of the curvature of a single asperity.

(2) The fractal asperity transition from elastic, elastoplastic to full plastic takes place in this order with an increase in the load and contact area.

(3) For determined material property and fractal parameters, the contact load is dependent on the biggest contact area of asperity and the critical elastic contact area.

(4) For constant characteristic length scale G, the slope of the load-area relation is proportional to the fractal dimension D. For constant fractal dimension D, the slope of the load-area relation is inversely proportional to G. For constant D and G, the slope of load-area relation is

inversely proportional to the property of the material ϕ.

References

[1] GREENWOOD J A, WILLIAMSON J B P. Contact of nominally flat surfaces[C]//*Proceedings of the Royal Society of London A: Mathematical, Physical and Engineering Sciences*, London, English, December, 1966, 295(1442): 300–319.

[2] CHANG W R, ETSION I, BOGY D B. An elastic-plastic model for the contact of rough surfaces[J]. *Journal of Tribology*, 1987, 109(2): 257–263.

[3] CIAVARELLA M, DELFINE V, DEMELIO G. A "re-vitalized" Greenwood and Williamson model of elastic contact between fractal surfaces[J]. *Journal of the Mechanics and Physics of Solids*, 2006, 54(12): 2569–2591.

[4] MAJUMDAR A, BHUSHAN B. Fractal model of elastic-plastic contact between rough surfaces[J]. *Journal of Tribology*, 1991, 113(1): 1–11.

[5] MAJUMDAR A, BHUSHAN B. Role of fractal geometry in roughness characterization and contact mechanics of surfaces[J]. *Journal of Tribology*, 1990, 112(2): 205–216.

[6] PENG Y F, GUO Y B. An elastic-plastic adhesion model for contacting fractal rough surface and perfectly wetted plane with meniscus[J]. *Chinese Journal of Mechanical Engineering,* 2009, 22(1): 9–14.

[7] MORAG Y, ETSION I. Resolving the contradiction of asperities plastic to elastic mode transition in current contact models of fractal rough surfaces[J]. *Wear*, 2007, 262(5): 624–629.

[8] KOGUT L, ETSION I. Elastic-plastic contact analysis of a sphere and a rigid flat[J]. *Journal of Applied Mechanics*, 2002, 69(5): 657–662.

[9] LIOU J L, LIN J F. A new microcontact model developed for variable fractal dimension, topothesy, density of asperity, and probability density function of asperity heights[J]. *Journal of Applied Mechanics,* 2007, 74(4): 603–613.

[10] LIOU J L, TSAI C M, LIN J F. A microcontact model developed for sphere- and cylinder-based fractal bodies in contact with a rigid flat surface[J]. *Wear,* 2010, 268(3): 431–442.

[11] LIOU J L, LIN J F. A modified fractal microcontact model developed for asperity heights with variable morphology parameters[J]. *Wear,* 2010, 268(1): 133–144.

[12] MIAO X M, HUANG X D. A complete contact model of a fractal rough surface[J]. *Wear*, 2014, 309(1): 146–151.

[13] CHEN Hui, HU Yuanzhong, WANG Hui, et al. Simulation and characterization of fractal rough surfaces[J]. *Chinese Journal of Mechanical Engineering*, 2006, 42 (9): 219–223. (in Chinese)

[14] SAYLES R S, THOMAS T R. Surface topography as a nonstationary random process[J]. *Nature*, 1978, 271(2): 431–434.

[15] YANG Hongping, FU Weiping, WANG Wen, et al. Calculation model of the normal contact stiffness of joints based on the fractal geometry and contact theory[J]. *Chinese Journal of Mechanical Engineering,* 2013, 49(1): 102–107. (in Chinese)

[16] JOHNSON K L. *Contact mechanics*[M]. Cambridge: Cambridge University Press, 1987.

[17] WANG S, KOMVOPOULOS K. A fractal theory of the interfacial temperature distribution in the slow sliding regime: Part II–Multiple domains, elastoplastic contacts and applications[J]. *Journal of Tribology*, 1994, 116(4): 824–832.

[18] HAN J H, SHAN P, HU S S. Contact analysis of fractal surfaces in earlier stage of resistance spot welding[J]. *Materials Science and Engineering*, 2006, 435(A): 204–211.

[19] JI CUICUI, ZHU HUA, JIANG Wei. Fractal prediction model of thermal contact conductance of rough surfaces[J]. *Chinese Journal of Mechanical Engineering*, 2013, 26(1):128–136.

[20] BHUSHAN B. The real area of contact in polymeric magnetic media–Ⅱ: Experimental data and analysis[J]. *ASLE Transactions*, 1985, 28(2): 181–197.

[21] WEI Long, LIU Heqi, ZHANG Penggao. Sliding friction surface contact mechanics model based on fractal theory[J]. *Chinese Journal of Mechanical Engineering*, 2012, 48(17): 106–113. (in Chinese).

Biographical notes

YUAN Yuan, born in 1978, is currently an associate professor at *Xi'an University of Technology, China*. He received his PHD degree from *Northwestern Polytechnical University, China*, in 2008. His research interests include rough surface mechanical properties, the tribology, the structure stability analysis and the fatigue life prediction.
E-mail: yuanytaurus@msn.com.

GAN Li, born in 1990, is currently a master candidate at *Xi'an University of Technology, China.* His research interests include rough surface mechanical properties.
Tel: +86-15829712487; E-mail: naiveagan@yeah.net.

LIU Kai, born in 1957, is currently a professor and a PhD candidate supervisor at *Xi'an University of Technology, China*. His research interests include mechanical transmission theory and application.
E-mail: kliu@mail.xaut.edu.cn.

YANG Xiaohui, born in 1979, is currently a PhD candidate and a senior engineer at *Xi'an Jiaotong University, China.* His main research interests include the structure stability analysis and the fatigue life prediction.
E-mail: yxh_fast@163.com